8. Momentum-Space Convergent-Close-Coupling Method for a Model e-H Scattering Problem

Igor Bray [1] and Andris Stelbovics [2]

[1] Electronic Structure of Materials Centre, The Flinders University of South Australia, G.P.O. Box 2100, Adelaide 5001, Australia
[2] Centre for Atomic, Molecular and Surface Physics, School of Mathematical and Physical Sciences, Murdoch University, Perth 6150, Australia

Abstract

The convergent-close-coupling (CCC) method is illustrated for the Temkin-Poet model of electron-hydrogen scattering. This model treats only states of zero orbital angular momentum, but has played an important role in the development and testing of methods of solution for general electron–atom scattering systems. This chapter describes the features of the model and discusses the application of the CCC approach to its numerical solution. All scattering processes: elastic, inelastic excitation, and ionization are found from a single unified calculation. The computer program associated with this chapter is the much reduced version of the general CCC code, but contains the essential techniques for solving large sets of coupled equations.

8.1 Introduction

The aim of this chapter is to introduce the reader to an approach for solving the coupled equations, which often arise in scattering theory, that is based on solving coupled integral equations in momentum space. The strength of the technique is that the linear integral equations have as their driving terms the Born approximations to the scattering amplitudes, thereby enabling higher-order perturbative approximations to be derived as iterative refinements in addition to the full integral-equation solution. The integral-equation system is readily solved by efficient algorithms which permit solution of relatively large sets of close-coupling equations.

In the past decade, enormous advances have been made in the theoretical modeling of electron–hydrogen scattering. It is the one problem in electron impact scattering theory we have been able to solve essentially without approximation and for which error bounds can be placed on scattering amplitudes over a wide range of energies. The reason for the recent progress has been the rapid development of the computing power available for the computational work. The close-coupling approach utilizes the fact that the complete set of eigenstates of the hydrogen atom (discrete plus continuum)

forms a basis for expanding the three-body electron-hydrogen wavefunction. An expansion of the wavefunction using the target states leads naturally to the desired asymptotic states of the system consisting of a plane wave for the incident electron and a hydrogen atom in one of the discrete states. Expanding the Schrödinger equation by means of these target states converts it to an (infinite system) of coupled equations which is formidable to solve directly because of the infinite sum over the discrete states and the integration over the continuum. However, it is physically reasonable to argue that at least at low incident electron energies, where the excited-state channels are closed, their contribution to the elastic scattering amplitudes should be small and this indeed is found to be the case. Thus early calculations truncated the target space to a few low lying excited states (hence the name "close-coupling") as these small-scale models were the only ones that were numerically tractable.

Subsequent studies gradually increased the target space subset by including, first, more target states and then square-integrable functions. The latter were not eigenstates but were chosen to span, efficiently, the remainder of the target space. These functions are now commonly called pseudo-states. A major effect of including these states, which approximate the higher discrete as well as continuum contributions, was to reduce the elastic cross section because of the additional loss of flux to these new channels. A new problem arose with the introduction of the pseudo-states. While they improved the agreement of theory with experimental data for many energies, the singlet scattering amplitudes developed unphysical resonances above the ionization threshold. These resonances are referred to as pseudo-resonances and their position and number vary with the number of the pseudo-state functions included in the expansions. In this next generation of models and calculations, ansatzes were used to average over the pseudo-resonances in order to produce smooth cross sections for elastic and inelastic scattering.

A parallel development occurred in the study of approximations to the spectrum of the hydrogen atom which has had a profound influence on shaping the present-day calculations. It is a standard result of mathematics that one can choose a set of Laguerre functions in such a manner as to form a basis for the Hilbert space of square-integrable functions. Yamani and Reinhardt [8.1] demonstrated that the hydrogen continuous spectrum (whose functions are not square integrable) could be expanded in such a basis in analytical form. They were also able to show that when a finite set of these functions was used, the resultant pseudo-states obtained from a diagonalization of the hydrogen-atom Hamiltonian in the subset, were just the Fourier expansions of the continuum restricted to the subspace. For the first time it was possible to understand the nature of the slow convergence of calculations which employ pseudo-states; they are a consequence of the slow convergence of the Fourier-series expansions of continuum states. A further important observation flowing from their analysis is that the completeness sum over the target wavefunctions calculated in a subspace of the Laguerre basis forms

a Gaussian quadrature approximation for the completeness relation of the exact discrete plus continuum states. This association of a quadrature rule with the discretization of the spectrum strongly suggests that a proper implementation of target-state expansions should utilize the complete set of approximate target states in order to obtain the full benefits of convergence accruing to the implicit quadrature rule. The present generation of calculations which incorporate these ideas and investigate convergence by systematically increasing the Laguerre subspace of the target are referred to as the convergent-close-coupling (CCC) method [8.2].

Rather than presenting the full complexity of the method applied to the full problem, we consider in this chapter the simpler problem, whereby the spectrum of the hydrogen target is restricted to S symmetry target states. Within this manifold the S states form a complete set and hence the ideas of the CCC method can be fully tested. It is also common but not essential to restrict the calculations to the $L = 0$ partial wave of the full three-body scattering wavefunction. Historically this model was first discussed by Temkin [8.3] and later by Poet [8.4] who used the specialized nature of the model to derive a highly accurate numerical solution which has evolved into a standard against which to check alternative methods. In this chapter we present the elements of the model, followed by a description of the Laguerre basis and then the method of solution of the CCC equations. Details of the use of the computer program are outlined through a number of examples.

8.2 Theory

The electron-hydrogen Schrödinger equation, for total energy E of the scattering system, is written as

$$(H - E)\,|\Psi^S\rangle = 0\,, \tag{8.1}$$

where the Hamiltonian operator is

$$H = K_0 + v_0 + K_1 + v_1 + v_{01}\,, \tag{8.2}$$

and the incident and target electrons are labeled 0 and 1 respectively. The proton is assumed static and infinitely heavy so $K_{0,1}$ refer to the electron kinetic energies, $v_{0,1}$ the electron-proton and v_{01} the electron-electron potentials. The three-body wavefunction $\Psi^S(\boldsymbol{r}_0, \boldsymbol{r}_1)$ is symmetric (singlet channel $S = 0$) or antisymmetric (triplet channel $S = 1$) as required by the Pauli exclusion principle. If the space of the target hydrogen atom is restricted to S states and further if only those collisions which result in zero total angular momentum are considered we have the Temkin-Poet model. In coordinate space the Schrödinger equation becomes

$$\left(\frac{1}{2}\frac{\partial^2}{\partial {r_0}^2} + \frac{1}{2}\frac{\partial^2}{\partial {r_1}^2} + \frac{1}{r_0} + \frac{1}{r_1} - \frac{1}{r_>} + E\right)\Psi^S(r_0, r_1) = 0, \tag{8.3}$$

where $r_> \equiv \max(r_0, r_1)$. Poet noted that if the domain was restricted to the region $r_0 > r_1$ the equation reduced to

$$\left(\frac{1}{2}\frac{\partial^2}{\partial {r_0}^2} + \frac{1}{2}\frac{\partial^2}{\partial {r_1}^2} + \frac{1}{r_1} + E\right)\Psi^S(r_0, r_1) = 0, \qquad r_0 > r_1. \tag{8.4}$$

This is of a separable form and has solutions comprising a plane wave in the coordinate r_0 and a Coulomb function in r_1. Of course the *physical solution* is formed by taking a superposition of these separable solutions which individually do not satisfy the physical boundary conditions. Poet showed that imposition of these boundary conditions along the boundary $r_0 = r_1$ lead to an integral equation which was much simpler to solve than the original differential equation. The interested reader is referred to the original paper [8.4] for details of his novel approach.

8.2.1 Close-Coupling Equations

The close-coupling method rewrites the Schrödinger equation (8.1) by making an expansion of the three-body wavefunction in terms of a complete set of target states of the hydrogen atom

$$(K_1 + v_1)|\phi_i\rangle = \epsilon_i|\phi_i\rangle. \tag{8.5}$$

The completeness of the states may be used to form an explicitly symmetrized expansion for the full wavefunction,

$$\Psi^S(\boldsymbol{r}_0, \boldsymbol{r}_1) = \frac{1}{2}\sum\!\!\!\!\!\!\int_i \left(\phi_i(\boldsymbol{r}_1)F_i^S(\boldsymbol{r}_0) + (-1)^S\phi_i(\boldsymbol{r}_0)F_i^S(\boldsymbol{r}_1)\right), \tag{8.6}$$

where the generalized summation indicates a summation over the discrete states and an integration over the continuum ones. By applying this expansion to (8.1) and folding on the left with target states, then using the orthogonality properties, the two-variable equation is replaced by a single variable system of coupled equations

$$\sum\!\!\!\!\!\!\int_i (K_0\delta_{ij} + V_{ji}^S)F_i^S = (E - \epsilon_j)F_j^S, \tag{8.7}$$

where

$$V_{ji}^S = \langle\phi_j|V^S|\phi_i\rangle = \langle\phi_j|v_0 + v_{01} + (-1)^S(H - E)P_r|\phi_i\rangle. \tag{8.8}$$

Here P_r is the space-exchange operator whose effect is to interchange r_0 and r_1. In this form the equations are still intractable because of the generalized summation over states. But they do have the advantage that they lend themselves to approximation schemes which allow them to be solved to high accuracy. One method we favor is to choose a finite subset of a countably infinite set of square-integrable (L^2) functions which form a basis for the hydrogen-atom Hilbert space.

8.2.2 Target-State Manifold

We choose the functions

$$\xi_i(r) = \left(\frac{\lambda(i-1)!}{(1+i)!}\right)^{1/2} (\lambda r)\exp(-\lambda r/2)L_{i-1}^2(\lambda r), \qquad i = 1, 2, \ldots, \quad (8.9)$$

which are L^2 and for $\lambda > 0$ form a basis for the target states with S symmetry. The $L_i^2(\lambda r)$ are associated Laguerre polynomials of order 2. Now, if we take the first N functions from the set (8.9) and diagonalize the hydrogen-atom Hamiltonian in this subspace we obtain a set of approximate eigenstates. Formally we can describe this process as one in which the Hamiltonian $H_1 = K_1 + v_1$ is replaced by $I^N H_1 I^N$ where I^N is the unit projection operator onto the subspace:

$$I^N = \sum_{i=1}^{N} |\xi_i\rangle\langle\xi_i|. \quad (8.10)$$

The eigenstates are defined by

$$I^N H_1 I^N |\phi_n^N\rangle = \epsilon_n^N |\phi_n^N\rangle, \quad \langle\phi_n^N|\phi_{n'}^N\rangle = \delta_{nn'}, \quad n = 1, 2, \ldots, N. \quad (8.11)$$

The pattern of eigenenergies is such that the lowest lying states are essentially exact with a reasonable choice for λ, while higher negative and positive energy states are a superposition of the true eigenstates, with greatest weighting from the nearby energies. One very useful effect of projecting onto a discrete subspace is to replace the integration over the continuum states by a summation. Indeed, if one pursues the nature of this further one can establish that the induced summation is equivalent to a Gaussian quadrature approximation to the generalized summation over the exact target states.

8.2.3 Ensuring the Uniqueness of Solution

The close-coupling equations (8.7) do not have a unique solution and this may therefore lead to numerical instabilities in their numerical solution. The reason for this is due to the form adopted for the symmetrized expansion in (8.6). It is best illustrated by taking an example from triplet (S=1) scattering. If F_i^1 is one solution, then so must be $F_i^1 + \alpha_i\phi_i$ for arbitrary constant α_i. The reason that the symmetrization procedure does not ensure uniqueness is because such an expansion is too general. The Pauli principle may be used once more to eliminate the non-uniqueness problem. This matter is discussed in detail elsewhere [8.2]. It may be shown that there are N^2 linearly independent spurious solutions for an N function subspace. Their elimination is deceptively simple; as a consequence of the Pauli principle, one finds that the additional condition

$$\langle\phi_i|F_j^S\rangle = (-1)^S\langle\phi_j|F_i^S\rangle \quad (8.12)$$

is necessary. Once this is implemented the solution may be demonstrated to be unique. The argument is tortuous so we merely state the result here. It is sufficient to replace the potential V^S by

$$V^S(\theta) = v_0 + v_{01} - E\theta I_0 + (-1)^S\big(H - E(1-\theta)\big)P_r. \tag{8.13}$$

Here I is the unit operator for the incident electron and θ is an arbitrary non-zero scalar. Since the solution does not depend on θ, a test of the numerical accuracy of a solution is obtained by repeating the calculation for several values of θ and ascertaining the variation in the numerical solution.

8.2.4 Momentum-Space Convergent-Close-Coupling

From now on, we assume that the target states and energies are those associated with the N-basis approximation defined in (8.11). In order to economize on notation the explicit dependence on N will be omitted from the equations where no confusion arises. A consequence of using the N-basis is that the generalized sum in the close-coupling equations (8.7) is replaced by a finite sum. This means that our scattering wavefunction will have an implicit dependence on N. However, as we already observed, the completeness relation over the subspace target states is a Gaussian quadrature approximation to the completeness relation over the exact target states. Hence one should expect convergence of the scattering wavefunction as N is increased using the Laguerre basis (8.9). This is the convergent-close-coupling (CCC) approach to calculation of electron-atom scattering. For ever increasing N we take the first N functions from the Laguerre basis and solve the resultant close-coupling equations until satisfactory convergence in the quantities of interest is obtained.

All of the information about the scattering processes is contained in scattering amplitudes which may be obtained from the scattering wavefunction $\Psi^S(r_0, r_1)$ matched to outgoing spherical-wave boundary conditions. There is a more direct way we can find the scattering amplitudes through use of a Lippmann-Schwinger equation for the **K** matrix and the closely associated **T** matrix. The momentum-space matrix elements of these operators,

$$\langle k'n'|K^S(E)|nk\rangle \equiv \langle k'|K^S_{n'n}(E)|k\rangle, \tag{8.14}$$

are directly related to the scattering amplitudes when the momenta k, k' are put on the energy shell in each open channel. We denote these on-shell momenta by k_n, $k_{n'}$. They satisfy the relation $\epsilon_n + \frac{1}{2}{k_n}^2 = \epsilon_{n'} + \frac{1}{2}{k_{n'}}^2 = E$. The **K** matrix operator is defined by

$$K^S(E) = V^S(E) + V^S(E)\mathcal{P}G_0(E)K^S(E), \tag{8.15}$$

where $\mathcal{P}G_0$ is a free Green's function with standing-wave boundary conditions. In momentum space this equation becomes a Fredholm integral equation of the second kind:

$$\langle k'n' \,|K^{SN} \mid nk_n\rangle = \langle k'n' \mid V^{SN}(\theta) \mid nk_n\rangle + \sum_{m=1}^{N} \mathcal{P} \int_0^\infty \mathrm{d}kk^2 \frac{\langle k'n' \mid V^{SN}(\theta) \mid mk\rangle}{E - \epsilon_m - \frac{1}{2}k^2} \langle km \mid K^{SN} \mid nk_n\rangle. \tag{8.16}$$

Note that we deliberately allow k' to be off the energy shell, as is k. This is necessary when solving this equation for the **K** matrix.

The integrand in (8.16) is singular when the momentum in the integration takes on the on-shell momentum for each open channel, but this singularity can be treated by numerical methods (see below). We note that the equation for **K** uses only real arithmetic and hence provides a considerable practical advantage over the corresponding **T** matrix Lippmann-Schwinger equation, which differs from that of the **K** matrix through the replacement of the standing-wave Green's function by one with outgoing wave boundary conditions. Unfortunately this has the effect of making the integral equation complex and hence complex arithmetic must be used to solve the system numerically, thereby requiring twice as much array storage. The on-shell **T** matrix elements, on the other hand, are obtained from the **K** matrix ones through the Heitler equation:

$$\langle k_{n'}n' \mid K^{SN} \mid nk_n\rangle = \sum_{m=1}^{N_{\mathrm{open}}} \langle k_{n'}n' \mid T^{SN} \mid mk_m\rangle \times \left(\delta_{mn} + \mathrm{i}\pi k_m \langle k_m m \mid K^{SN} \mid nk_n\rangle\right). \tag{8.17}$$

The sum in the above equation only extends over the open channels.

8.2.4 Cross Sections

We define the spin-dependent cross section for excitation from an initial state n to a final state n' in atomic units (a_0^2) as

$$\sigma_{n'n}^{SN} = (2S+1)\pi^3 \frac{k_{n'}}{k_n} \left|\langle k'n'|T^{SN}|kn\rangle\right|^2, \tag{8.18}$$

with the spin-averaged cross section being given by the sum of the $S = 0$ and $S = 1$ cross sections. The total cross section for excitation from initial state n is obtained by either summing over individual cross sections or by the use of the optical theorem,

$$\sigma_{\mathrm{Tot}\ n}^{SN} = \sum_{n'=1}^{N_{\mathrm{open}}} \sigma_{n'n}^{SN} = -\pi^2(2S+1)\mathrm{Im}(\langle k'n'|T^{SN}|kn\rangle)/k. \tag{8.19}$$

We define the total ionization cross section by summing that subset of excitations which lead to final states in which both the scattered and excited electron target have positive energies, i.e.,

$$\sigma^{SN}_{\mathrm{Ion}\ n} = \sigma^{SN}_{\mathrm{Tot}\ n} - \sum_{n':\epsilon_{n'}<0}^{N_{\mathrm{open}}} \sigma^{SN}_{n'n} = \sum_{n':\epsilon_{n'}>0}^{N_{\mathrm{open}}} \sigma^{SN}_{n'n}. \tag{8.20}$$

When only a few states are used we may take more care to ensure that there is no contribution to the estimated ionization cross section from the discrete subspace by projecting the total non-breakup cross section ($\epsilon_{n'} < 0$) onto the true discrete subspace, formed using exact hydrogen eigenstates.

It is important to make it clear what we mean by convergence with increasing N. Suppose we require a cross section to a specified accuracy ε. Then we say we have convergence at $N = N_0$ if for $N > N_0$ we have $|\sigma^{SN}_{n'n} - \sigma^{SN_0}_{n'n}| < \varepsilon$. In practice we use the converse procedure, where by presenting a set of results for various N we are able to give an estimate of ε and hence of the accuracy of our calculations. The rate of convergence, the values of N_0 and ε all depend on the transition of interest, total spin, and the incident energy. Typically, the least detailed and largest cross sections are the easiest to obtain accurately. On the other hand, individual **T** matrix elements are the slowest to converge, particularly when small.

8.3 Numerical Solution

The required computation may be split into three parts. First we need to diagonalize the target Hamiltonian using our chosen Laguerre basis. We then need to calculate the fully off-shell **V** matrix elements for the various channel combinations. And finally, we form and solve a set of linear equations yielding half-on-shell **K** matrices. These are then used to form the on-shell **K** matrices, which are in turn used to generate the on-shell **T** matrix elements and cross sections.

8.3.1 Diagonalizing the Target Hamiltonian

We wish to obtain states $\langle r|n\rangle \equiv \phi_n(r)/r$ which are linear combinations of our basis functions $\xi_i(r)$ (see (8.9-11)) and satisfy

$$\langle n|H_1|n'\rangle = \delta_{nn'}\epsilon_n. \tag{8.21}$$

In other words, we wish to find the eigenvalues and eigenvectors of H_1 within the Hilbert subspace spanned by the N orthonormal basis functions. To do this we write

$$0 = \langle \xi_n|\epsilon_{n'} - H_1|n'\rangle = \sum_{m=1}^{N} \big(\delta_{nm}\epsilon_{n'} - \langle \xi_n|H_1|\xi_m\rangle\big)c_{mn'}, \tag{8.22}$$

where

$$|n'\rangle = \sum_{m=1}^{N} c_{mn'}|\xi_m\rangle. \tag{8.23}$$

This forms a standard eigenvalue problem that we solve using the `LINPACK` routine `RS`. The coefficients $c_{mn'}$ depend on the subspace dimension N. The major difficulty in this process is calculating the matrix elements of the target Hamiltonian H_1 using the specified basis. We leave it to the interested reader as an exercise to evaluate analytical expressions for these matrix elements.

8.3.2 Calculating V Matrix Elements

We wish to calculate matrix elements of the form

$$\begin{aligned}
&\langle k'n'|\frac{1}{r_>}-\frac{1}{r_0}-EI_0^N\theta+(-1)^S(H_0+H_1+\frac{1}{r_>}-E(1-\theta))P_r|nk\rangle \\
&\quad=\langle n'k'|\frac{1}{r_>}-\frac{1}{r_0}+(-1)^S\frac{1}{r_>}P_r|nk\rangle-\delta_{n'n}E\theta\sum_{m=1}^{N}\langle k'|m\rangle\langle m|k\rangle \\
&\qquad+(-1)^S\Bigg[\left(\frac{k^2}{2}+\frac{k'^2}{2}-E(1-\theta)\right)\langle k'|n\rangle\langle n'|k\rangle \\
&\qquad\quad-\langle k'|\frac{1}{r}|n\rangle\langle n'|k\rangle-\langle k'|n\rangle\langle n'|\frac{1}{r}|k\rangle\Bigg]. \qquad (8.24)
\end{aligned}$$

Only the first part of (8.24) is not trivial, so we will write it out explicitly:

$$\begin{aligned}
\langle k'n'|\frac{1}{r_>}-\frac{1}{r_0}|nk\rangle&=\frac{2}{\pi kk'}\int_0^\infty \mathrm{d}r_0\sin(k'r_0)\sin(kr_0) \\
&\quad\times\left[\left(\int_0^{r_0}\frac{\mathrm{d}r_1}{r_0}+\int_{r_0}^{\infty}\frac{\mathrm{d}r_1}{r_1}\right)\phi_{n'}(r_1)\phi_n(r_1)-\frac{\delta_{nn'}}{r_0}\right] \qquad (8.25)
\end{aligned}$$

and

$$\begin{aligned}
\langle k'n'|\frac{1}{r_>}P_r|nk\rangle&=\frac{2}{\pi kk'}\int_0^\infty \mathrm{d}r_0\sin(k'r_0)\phi_n(r_0) \\
&\quad\times\left(\int_0^{r_0}\frac{\mathrm{d}r_1}{r_0}+\int_{r_0}^{\infty}\frac{\mathrm{d}r_1}{r_1}\right)\phi_{n'}(r_1)\sin(kr_1). \qquad (8.26)
\end{aligned}$$

Note that square-integrability of our states $\phi_n(r)$ ensures the existence of all of the integrals. We evaluate the $\mathbf{V}$ matrix elements for all channel (n, n') combinations and various values of k and k'.

Another important point to consider is the consequence of choosing a non-zero θ in (8.24). Such a choice introduces the $\langle k'|I^N|k\rangle$ term which tends to $\delta(k-k')$ with increasing N. Therefore, the integration over k' becomes increasingly more difficult (more quadrature points are necessary) as N is increased. This is unfortunate, as the size of the calculations grows more

rapidly than if just N is increased. Fortunately in the case of the Temkin-Poet model, the on-shell results remain stable even for the $\theta = 0$ case. These issues will be discussed in more detail later on.

8.3.3 Solution of the Coupled Equations

We now discuss the numerical techniques used in solving the coupled integral equations. Here we restrict ourselves to the simple Temkin-Poet model of electron-hydrogen scattering but the method of solution is general. For example, the same techniques may be used for calculating scattering of electrons from general multi-electron targets. To date they have been applied to one-electron atoms and ions [8.5], as well as helium [8.6]. The only differences are that the size of the matrices is larger due to the inclusion of target states of general angular momenta and that we have to solve the coupled equations for many partial waves.

Another important point is that the momentum-space method of solution of the coupled equations will yield very similar results to the intermediate energy **R** matrix (IERM) method [8.7,8.8] or variational approaches [8.9] involving coupled integro-differential equations, assuming a similar level of sophistication in describing the target states. Because convergent amplitudes are obtained only by solving large sets of coupled equations, a key issue is that of solving them with maximum efficiency. The momentum-space method discussed here can be implemented on desk-top workstations, making it accessible to a large audience. This quest for efficiency has been paramount in our design of the codes.

8.3.3.1 Formation of the Linear Equations

Our first step is to discretize the integral (8.16) by taking a quadrature rule for the integration from zero to infinity. Choosing an efficient quadrature grid is very important as this leads to smaller matrices. However, this process is complicated by the fact that we have a principal-value type singularity whose position varies with the channel energy ϵ_n. Only open channels have the singularity. For closed channels the denominator remains negative for all values of k.

We deal with this problem by breaking the integration range into a number of parts with the boundaries being chosen dependent on the position of the singularity, if any. Generally, we have N_{k_1} Gaussian points in the interval $(0,k_1)$, N_{k_2} points in the interval (k_1, k_2) and N_{k_3} points in the interval (k_2, ∞). For those channels that contain the singularity we take an additional even number (N_{k_4}) of Gaussian points in an interval of width w positioned symmetrically about the singularity. This is an efficient way of dealing with this type of singularity. In order to complete the quadrature rule to infinity we suppose that the integrand falls off as k^{-p} for $k > k_2$.

Upon the replacement of the integral in channel m by a quadrature rule using N_m points with weights w_{jm} $(j = 1, \ldots, N_m)$, we may write (8.16) as

$$\langle k'n'|K^{SN}|nk\rangle = \langle k'n'|V^{SN}(\theta)|nk\rangle + \sum_{m=1}^{N}\sum_{j=1}^{N_m} \frac{w_{jm}k_{jm}^2\langle k'n'|V^{SN}(\theta)|mk_{jm}\rangle\langle k_{jm}m|K^{SN}|nk\rangle}{E-\varepsilon_m-k_{jm}^2/2}, \quad (8.27)$$

or in matrix notation as

$$K^{SN}(k_{j'n'},n) = V^{SN}(k_{j'n'},n,\theta) + \sum_{jm} W_{jm}V^{SN}(k_{j'n'},k_{jm},\theta)K^{SN}(k_{jm},n), \quad (8.28)$$

where we included the energy denominator in the new generalized weights W_{jm}. In order to solve (8.28) we allow the $k_{j'n'}$ to run over the same range as the k_{jm} and form a set of linear equations of the form $AX = B$, where the square matrix **A** is given by $A = I - WV^{SN}(\theta)$, and $B = V^{SN}(n,\theta)$ and $X = K^{SN}(n)$ are vectors. I is the identity matrix and W is the diagonal matrix with entries W_{jm}. For compactness of notation, we omitted the entrance channel momentum since it is fixed to the on-shell value.

Now let us consider the optimal choice of quadrature rule in (8.27) above. We mentioned that the introduction of non-zero θ in the **V** matrix elements leads to a δ-function-like term. The quadrature rule must be able to integrate accurately over such terms. In particular, we need to make sure that we are able to integrate with respect to k' over terms like $\sum_m \langle m|k'\rangle$. The quality of the channel-dependent quadrature rule may be tested independently of doing the full calculation by checking that $\int \mathrm{d}k'\langle m|k'\rangle\langle k'|m\rangle = 1$ to sufficient precision for each m.

8.3.3.2 Solution of Linear Equations

It is the maximum size of the matrix **A**, for a given set of computational resources, that determines the number of coupled equations that we may solve. The matrix **A** must fit into the core memory as the time required to solve the linear equations of a $n \times n$ system is proportional to n^3, and so takes a considerable part of the computational time. To minimize storage requirements we take advantage of the fact that $V^{SN}(k_{j'n'},k_{jn},\theta)$ is symmetric upon interchange of $j'n'$ and jn and that for electron impact excitation we may have at most two possible total spins S (S=0,1 in the case considered here). As a result we are able to use the same matrix, of dimension $n\times(n+1)$ for storing the **V** matrix elements for both spins. The extra dimension is so that there is room for both the diagonals of the S=0,1 cases.

Having stored the **V** matrix elements efficiently, we rewrite the linear equation $AX = B$ in such a way so that the matrix **A** is symmetric. This is achieved by writing (8.28) as

$$(IW^{-1} - V^{SN}(\theta))WK^{SN}(n) = V^{SN}(n,\theta). \quad (8.29)$$

Thus we are able to form **A** using the same array that is used for storage of the **V** matrix elements. Using the `LAPACK` routine `SSYSV`, we may solve

the linear equations separately for the two spin channels using only the space provided for the matrix **A**. After solution of the linear equations for each total spin, the corresponding **V** matrix elements are destroyed, since they are no longer necessary. Note that we do need to save the half-on-shell **V** matrix elements prior to the solution of the linear equations, which take very little space.

In summary, we are able to solve the coupled equations using primarily only the space necessary for storing the fully-off-shell **V** matrix elements for the two spin cases. This efficient usage of memory has enabled the CCC method to solve large sets of close-coupling equations using relatively inexpensive desk-top computational resources. (See, for example, Bray [8.10].)

8.4 Computer Program

The program associated with this chapter is a much reduced version of the CCC program used to calculate electron or positron scattering on hydrogen-like and helium-like atoms and ions. For the sake of simplicity and compactness, the reduced version applies only to the Temkin-Poet model. In other words, the target states are the S states of hydrogen, and only the $\ell = 0$ partial-wave of the projectile is treated.

The file `README` contains the information on the associated source codes and on how to make the run-file `ccc`.

8.4.1 Input

There is a single input file `ccc.in` with four lines containing the following input parameters:

1. `ENERGY, NZE, NATOP, NPS, ALPHA`

`ENERGY` Incident energy (eV) on the ground state. It may range from approximately 0.1 eV to 1000 eV.

`NZE` -1 for electron scattering
1 for positron scattering.

`NATOP` Normally the number of states to be coupled. For convenience it may be used as a switch to make the size of the Laguerre basis determine the number of states to be coupled. A value of 0 means all `NPS` states will be coupled. A value of $-n$ means that all open plus $-n+1$ closed states will be coupled.

`NPS` $= N$, the size of the Laguerre basis that generates `NPS` states.

`ALPHA` Exponential fall-off factor of the Laguerre basis, $\alpha = \lambda/2$.

2. `NUNIT, NNBTOP, NENT, IFIRST, NOLD, THETA`

`NUNIT` 1 for the cross section units to be in a_0^2;
2 for πa_0^2;
3 for cm^2.

`NNBTOP` Used to form overlaps between the first `NNBTOP` exact hydrogen discrete S states and those obtained by diagonalization.
`NENT` Number of entrance channels.
`IFIRST` 1 if direct and exchange is to be calculated;
0 for the direct case only.
`NOLD` 1 for the case of using the Laguerre-basis states;
0 for using the exact discrete states.
`THETA` Parameter that, when non-zero, ensures uniqueness of the solution of the Lippmann-Schwinger equation.

3. `NQM, QCUT, RMAX, SLOWE`

`NQM` -1 for using the full set of k integration points;
1 for a unitarized Born approximation.
`QCUT` Determines the spacing in the coordinate space mesh. For $q <$ `QCUT`, $\sin(qr)$ will be reliably integrated.
`RMAX` Largest value in the coordinate mesh.
`SLOWE` If non-zero, then `ALPHA` is iterated until one of the pseudo-states has `SLOWE` as the energy.

4. `(NK(I),SK(I),I=1,4)`

These are the k-grid parameters that are used to distribute the k integration points in each channel.
`NK(1)` Number of points in the interval (0,`SK(1)`);
`NK(2)` Number of points in the interval (`SK(1)`,`SK(2)`);
`NK(3)` Number of points in the interval (`SK(2)`,∞);
`SK(3)` Power p used to define the distribution of points in the last interval.
`NK(4)` Number of extra points distributed about the on-shell point, if any, and lying inside one of the previous intervals. This number must be even.
`SK(4)` Half the width w of the interval containing the singularity, if any. See the output for the actual distribution of points.

In addition to the above input parameters, there are a set of parameters in the file `par.f` which control the sizes of available arrays. Informative messages are returned if the array sizes are exceeded. The major requirements of memory are the array `VMAT` in which the $\mathbf{V}$ matrix is stored, and the array `CHIL` in which the plane waves ($\sin(kr)$) are stored. The array `VMAT` requires space for (`KMAX * NCHAN`)^2 real numbers, where `KMAX` is the maximum number of k-grid points in any channel, and `NCHAN` is the maximum number of channels (or states). The array `CHIL` requires space for `KMAX * NCHAN * MAXR` real numbers, where `MAXR` is the maximum number of r-integration points.

8.4.2 Output

There is standard output which monitors the progress of the program as well as the creation of the files `totalcs`, `singlet.`n`1`, and `triplet.`n`1`. The file

`totalcs` presents the total cross sections. The `singlet.`n`1` and `triplet.`n`1` files contain the half-on-shell **K** and **V** matrix elements for the excitation of the initial channel to channel n. These are useful for making plots to show uniqueness, or lack thereof, in the solution of the Lippmann-Schwinger equations.

8.4.2.1 Standard Output
The standard output displays the set of states used in the multi-channel expansion. All of the states arising out of the diagonalization of the target Hamiltonian are listed. Those to be included in the multi-channel expansion have a "+" in the final column. The negative energy states are projected onto the true discrete subspace, using the earlier calculated hydrogen bound states. This projection is used when forming ionization cross sections. The results, given in the `totalcs` file, differ significantly from (8.20) only when very few states are used.

After presenting the target state information, the distribution of the k integration points is given in each channel m. A "$*$" appearing in an interval indicates that the singularity is in this interval. The tests consist of checking that $\int_0^\infty \mathrm{d}k k^2 |\langle m|k\rangle\langle k|m\rangle| = 1$. Each channel-dependent integration grid is tested with all $m = 1, \ldots, N$. The variable `NBAD` indicates how many tests did not yield unity to better than three significant figures. This is only a rough indication of the quality of the k quadratures. In the final analysis, a number of calculations must be run with varying distribution and number of k points to ensure accuracy of the final results.

After the k-grids have been set up and displayed, the **V** matrix elements are calculated, followed by the formation and solution of the coupled Lippmann-Schwinger equations. The final on-shell **T**, **S**, **K**, and **V** matrix elements are then printed out. Eigenphases and their sums are also given.

8.4.2.2 The file `totalcs`
The `totalcs` file contains the integrated cross sections. The following abbreviations are used. `TNBCS` is the total non-breakup cross section and is evaluated by summing the integrated cross sections for negative energy states. `TICS` is the total ionization cross section which is initially evaluated by simply summing the cross sections for positive energy states. Finally, it is estimated by subtracting from the total cross section (`TCS`) the cross sections from states with negative energies multiplied by the corresponding projection. The spin asymmetry is also given.

8.4.2.2 The files `singlet.`n`1` and `triplet.`n`1`
These are plot files containing the half-off-shell $K(k)$ and $V(k,\theta)$ matrix elements for the $1 \to n$ transition. These are the first two vectors in (8.28). Suppose we have two calculations which only vary in their k-grid parameters. Then we would expect that the two corresponding half off-shell $K(k)$ and $K(k')$, and $V(k,\theta)$ and $V(k',\theta)$ vectors should interpolate smoothly. Furthermore, one would expect that a particular $V(k,\theta)$ generates a unique

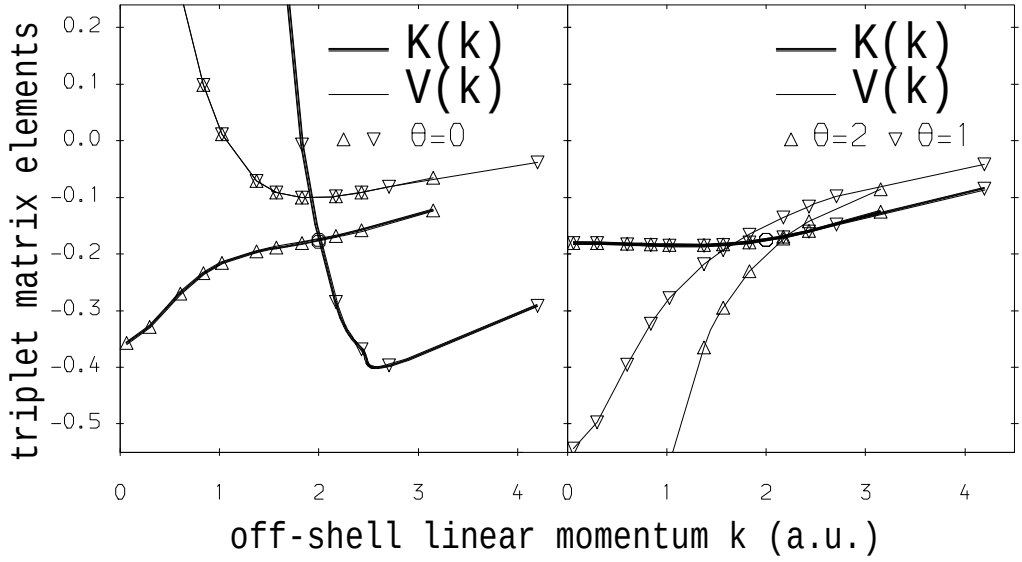

Fig. 8.1. Half-off-shell triplet **V** and **K** matrix elements arising in the static-exchange model of e-H scattering are shown for the "old" CC equations ($\theta = 0$), and the "new" form with $\theta = 1, 2$. The two integration k-grids (upright and inverted triangles) differ only in the last few points. The incident energy of 54.42 eV corresponds to the on-shell value of $k = 2$ atomic units (denoted by $\circ$). The lines connecting the points are provided as a visual guide.

$K(k)$, whereas another $V(k, \theta')$ yields $K'(k)$. For the $\theta = 0$ case, we find that two different k-grids generate distinct $K(k)$ and $K'(k')$, but $K(k_f) = K'(k_f)$ if k_f is the on-shell point. However, in the case of $\theta \neq 0$ two distinct $V(k, \theta)$ and $V(k, \theta')$ yield identical vectors $K(k)$ and $K'(k)$.

These ideas may be illustrated by taking the static-exchange model of electron-hydrogen scattering. In this model, only the single physical $(1s)^2S$ state is included in the close-coupling expansion. The question of uniqueness may then be studied in the triplet channel only. Looking at the **V** matrix elements (8.24) reveals that the θ term disappears for $S = 0$, but remains for the triplet ($S = 1$) channel. Figure 8.1, from [8.11], gives this example. In the left picture, we have two k-grids that only differ in their last two points. Yet the difference between the two resulting half-off-shell **K** matrix elements is enormous. However, the two curves do intersect at the on-shell point. In the right picture, we keep the same k-grids but perform calculations for different non-zero values of θ. We see that though the **V** vectors are quite different they yield the same **K** vectors. This demonstrates how any non-zero θ ensures uniqueness of the solution of our coupled equations.

In practice, for large-scale calculations, the use of a non-zero θ is crucial for obtaining numerically stable results. In the case of the simple model considered here, we find that both cases lead to reliable on-shell results. For reasons outlined above, the $\theta = 0$ case often requires fewer k points to solve for the on-shell matrix elements of the Temkin-Poet model — considerably fewer in the case of a relatively large basis size N (20 or so).

8.4.2.3 Sample Input and Output
A sample input file `book.in`, given together with the source code, has the following input parameters:

```
16.0,-1,0,5,0.5   ENERGY, NZE, NATOP, NPS, ALPHA
2,5,1,1,1,0.5     NUNIT, NNBTOP, NENT, IFIRST, NOLD, THETA
-1,8.0,100.0,2.0  NQM, QCUT, RMAX, SLOWE
14,0.9,22,3.0,4,4.0,10,0.2 (NK(I),SK(I),I=1,4) K grid params
```

which yields, in part, the following output:

```
 JS f i  real(T)   imag(T)    real(S)   imag(S)
 0+ 1 1-1.213E-01-1.061E-01  2.770E-01 8.266E-01
 0+ 2 1-7.162E-02 2.502E-02  1.323E-01 3.786E-01
 0+ 3 1-4.349E-02 1.976E-02  9.364E-02 2.060E-01
 0+ 4 1 5.527E-02 2.798E-02  7.556E-02-1.493E-01
 N=  240 eigenphase sum: -1.401
 0- 1 1-7.067E-02-2.749E-01 -8.733E-01 4.815E-01
 0- 2 1-8.361E-03-1.035E-02 -5.472E-02 4.419E-02
 0- 3 1-2.077E-04-4.301E-03 -2.038E-02 9.839E-04
 0- 4 1-1.423E-03 2.710E-03  7.317E-03 3.844E-03
 N=  240 eigenphase sum:  1.856
```

Here the singlet case is denoted by + and the triplet case by −. The S wave is denoted by $J = 0$.

8.4.3 Typical Usage

Typically the program is used to find the singlet and triplet 1s→ ns cross sections for the Temkin-Poet model at a particular energy. The rate of convergence with basis size N depends on the energy E, spin S, and principal quantum number n. If we are interested in the case $n \leq 2$ we may start with $N = 10$ and $\alpha = 0.5$. This yields a good representation of both the discrete and the continuum subspaces.

A more general usage of the program is to run it several times over a range of energies to see if the resultant cross sections are smooth or if pseudo-resonance behavior is evident. Pseudo-resonances are typically associated with pseudo-thresholds. To make this study particularly convenient,

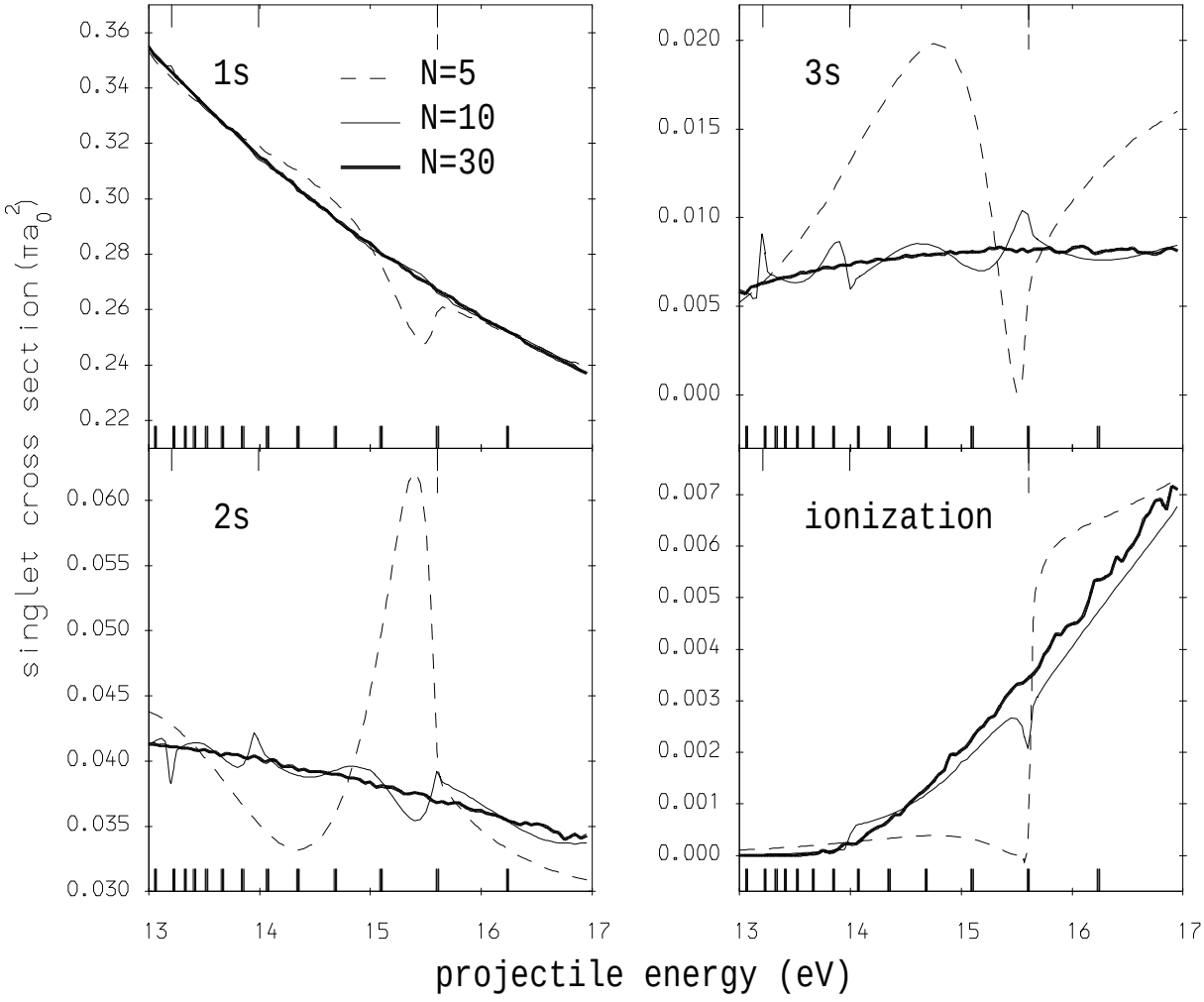

Fig. 8.2. The 1s, 2s, 3s, and ionization singlet cross sections in the Temkin-Poet model are shown in a small energy range for three basis sizes. The large tick marks on the horizontal axes indicate energy thresholds corresponding to the indicated basis size. For a given projectile energy E, states corresponding to thresholds less than E are open, those greater than E are closed. The exponential fall-off factor λ has been varied so that all three basis sizes have a state with energy 2 eV, leading to a common pseudo-threshold at 15.6 eV.

therefore, we have incorporated an iterative process which varies `ALPHA` to ensure that one of the target-state energies comes out to be `SLOWE`. This results in a fixed pseudo-threshold, irrespective of N, thereby allowing for a detailed study of cross sections in its vicinity. Such a study is shown in Fig. 8.2, also presented in [8.11]. Here we have set `SLOWE` = 2 eV for all three values of $N = 5, 10, 30$, resulting in a common pseudo-threshold at 15.6 eV. In the energy range considered, there is only one pseudo-threshold for the $N = 5$ case, three in the case of $N = 10$, and fourteen in the case of $N = 30$. The energy of the projectile determines which of the pseudo-states may be genuinely excited. The pseudo-thresholds below the projectile energy generate open channels, whereas the other channels are closed. In the case of $N = 5$ and $N = 10$, we see that associated with each pseudo-threshold is a pseudo-resonance in the cross section, which substantially diminishes in magnitude and width with increasing N. The significance of the above results is that pseudo-resonances are a manifestation of an insufficiently large N, though accurate answers may still be obtained if a little care is exercised when using small N to ensure that there are no nearby pseudo-thresholds.

8.5 Summary

We have given a brief outline of the simplified model of electron-hydrogen scattering that treats only states with zero orbital angular momentum. The strength of this model is that treatment of exchange and the continuum must be accurate in order to obtain reliable results. One of the very first applications of the CCC method was to this model. We were able to demonstrate conclusively that the continuum may be treated systematically by the use of square-integrable states. The program, associated with this chapter, allows the reader to verify this for themselves. The program presented here is limited to this restricted model. However, all of the successes of the CCC method in full scattering problems, including ionization, are due to the success of the method for this simple model. Applications of the method to calculations of realistic problems are discussed in several of the references.

8.6 Suggested Problems

The program is a substantially reduced version of the general code for one-electron targets, for the sake of simplicity. In order to make it applicable to real problems a number of extensions are necessary. The following list provides a series of suggestions for extending the code to the general case. The numbered items are graded in order of increasing complexity.

1. Copy the file `book.in` to `ccc.in`, run the `ccc` program, and check the output against the file `book.out`. Note that the input `ALPHA` has been iterated to obtain a pseudo-state with energy 2 eV. Check that the resultant `totalcs` file contains the 16 eV singlet cross sections given in Fig. 8.2.

2. Reproduce the plotted data for `THETA` = 0 of Fig. 8.1 by using, in turn, the two given input examples `kgrid1.in` and `kgrid2.in`. The required data are created in the corresponding `triplet.11` files. Edit the input files to vary `THETA` and reproduce data presented on the right side of Fig. 8.1. Choose other values of `THETA` and check for stability of the **K** matrix elements and variation of the **V** matrix elements.
3. We have discussed convergence of the on-shell **K** matrix elements with increasing basis size N. Check for convergence of the half-off-shell **K** matrix elements. This is discussed in ref. [8.11]. Begin with the `book.in` file and increase `NPS`. For large `NPS` you may need to take more care with the k-grids and/or change `THETA` to zero.
4. The unitarized Born approximation (UBA) for the **T** matrix is often used as a high energy approximation in electron scattering. It is obtained from the Heitler equation (8.17) by replacing the **K** matrix terms by the on-shell potentials. Work out an explicit form for the UBA **T** matrix.
5. If one iterates the **K** matrix equation (8.15) one obtains the series $K = V + VG_0V + VG_0VG_0V + \ldots$ Show that the second-order approximation to the **K** matrix requires only on-shell and half-on-shell potentials. You should find it relatively easy to develop an algorithm from (8.28) to do this numerically.
6. What new feature is needed to extend the second-Born calculation to arbitrary order? If you calculate the higher-order approximations you are not guaranteed to converge to the same answer you get by solving the set of linear equations (8.29). You may find that convergence is absent even in the high-energy limit. The interested reader is referred to [8.12] for further details.
7. The solution of the Lippmann-Schwinger equation discussed here assumed a plane-wave formalism. A distorted-wave formalism may be used instead. Derive a distorted-wave version of the close-coupling equations, see [8.5]. In this case the driving term of the linear equations becomes more dominant, thereby reducing the difficulty of solution of the coupled equations.
8. The implementation of the distorted-wave formalism also allows for extending the program code to ionic targets. Note that a major change is required in the construction of the channel Green's functions in the kernels. Can you explain why? See reference [8.5] for a full discussion of this point.
9. For incorporation of target states with arbitrary angular momentum the Laguerre function set (8.9) must be be modified. What would be a suitable modification? See [8.2] for details. This generality has been left in the existing code; see routine `MAKEPS`.
10. Calculation of the higher ℓ projectile angular momenta must be added to describe the collision generally. Assuming LS coupling holds, write down the form of the general partial-wave three-body wavefunction expanded

in terms of a complete set of target states coupled to general projectile states.

11. Incorporation of non-zero angular momentum states leads to more complicated **V** matrix elements. Using your answer to problem 10, derive an expression for the general momentum-space matrix element. For the case of hydrogenic targets this may be found in [8.5], for the case of helium in [8.6].

References

8.1 H.A. Yamani and W.P. Reinhardt, Phys. Rev. A **11** (1975) 1144
8.2 I. Bray and A.T. Stelbovics, Phys. Rev. A **46** (1992) 6995
8.3 A. Temkin, Phys. Rev. A **126** (1962) 130
8.4 R. Poet, J. Phys. B **11** (1978) 3081
8.5 I. Bray and A.T. Stelbovics, Adv. At. Mol. Opt. Phys. **35** (1995) 209
8.6 D.V. Fursa and I. Bray, Phys. Rev. A **502** (1995) 1279
8.7 M.P. Scott, T.T. Scholz, H.R.J. Walters and P.G. Burke, J. Phys. B **22** (1989) 3055
8.8 T.T. Scholz, H.R.J. Walters, P.G. Burke and M.P. Scott, J. Phys. B **24** (1991) 2097
8.9 Y.D. Wang and J. Callaway, Phys. Rev. A **50** (1994) 2327
8.10 I. Bray, Phys. Rev. A **49** (1994) 1066
8.11 I. Bray and A.T. Stelbovics, Comp. Phys. Comm. A **85** (1995) 1
8.12 A.T. Stelbovics, Phys. Rev. A **41** (1990) 2536